ACI MATERIALS JOURNAL TECHNICAL PAPER

Title no. 88-M46

Size Effect in Fatigue Fracture of Concrete

by Zdeněk P. Bažant and Kangming Xu

Crack growth caused by load repetitions in geometrically similar notched concrete specimens of various sizes is measured by means of the compliance method. It is found that the Paris law, which states that the crack length increment per cycle is a power function of the stress intensity factor amplitude, is valid only for one specimen size (the law parameters being adjusted for that size) or asymptotically, for very large specimens. To obtain a general law, the Paris law is combined with the size-effect law for fracture under monotonic loading, proposed previously by Bažant. This leads to a size-adjusted Paris law, which gives the crack length increment per cycle as a power function of the amplitude of a size-adjusted stress intensity factor. The size adjustment is based on the brittleness number of the structure, representing the ratio of the structure size d *to the transitional size* d_o *which separates the responses governed by nominal stress and stress intensity factor. Experiments show that* d_o *for cyclic loading is much larger than* d_o *for monotonic loading, which means that the brittleness number for cyclic loading is much less than that for monotonic loading. The crack growth is alternatively also characterized in terms of the nominal stress amplitude. In the latter form, the size effect vanishes for small structures while, in terms of the stress intensity factor amplitude, it vanishes for large structures. The curves of crack length versus the number of cycles are also calculated and are found to agree with data.*

Keywords: concretes; crack propagation; cyclic loads; **fatigue (materials); fracture properties;** loads (forces); tests.

The evolution of cracking in concrete structures requires rational modeling to obtain more reliable predictions of structural response to earthquake, traffic loads, environmental changes, and various other severe loads. Repeated loading causes cracks to grow. This phenomenon, called fatigue fracture, has been studied extensively for metals[1-3] and ceramics[4-6] and is now understood relatively well. For concrete, however, the knowledge of fatigue fracture is still rather restricted. Aside from fatigue studies outside the context of fracture mechanics,[7-11] experimental investigation of fracture under cyclic loading has been limited.[12-16] These investigations indicated that application of the Paris law for crack growth under repeated loading [17,18] can, at least to some extent, be transferred from metals to concrete. However, one important aspect—size effect—has apparently escaped attention so far where fatigue is concerned.

The objective of the present study is to investigate size effect, both experimentally and theoretically. Microstructural mechanisms[4-6] are beyond the scope of this investigation. The main goal is to identify the global (first-order) approximate description of the deviations from linear elastic fracture mechanics and Paris law.

FATIGUE TESTS OF SIMILAR NOTCHED BEAMS OF DIFFERENT SIZES

Two series of three concrete three-point-bend beam specimens of different sizes were tested in a closed-loop servo-controlled testing machine (see Fig. 1 and 2). The ratio of cement:sand:aggregate:water in the concrete mix was 1:2:2:0.6, by weight. The aggregate was crushed limestone of maximum size 0.5 in. (12.7 mm). The sand was siliceous river sand passing through sieve No. 1 (5-mm). Type I portland cement with no admixtures was used. From each batch of concrete, three beam specimens of different sizes (one of each size) were cast, along with companion cylinders of diameter 3 in. (76.2 mm) and length 6 in. (152 mm) for strength measurement. After the standard 28-day curing of the companion cylinders, their mean compression strength was $f_c' = 4763$ psi (32.8 MPa), with a standard deviation of 216 psi (1.49 MPa). The average direct tensile strength (which, however, is not needed for the present formulation) may be estimated as $f_t' = 6\sqrt{f_c'}$ psi = 414 psi (2.86 MPa), and Young's elastic modulus as $E = 57{,}000\sqrt{f_c'}$ psi = 3.93×10^6 psi (27,120 MPa). An additional series of nine notched beam specimens of three different sizes, three of each size, was cast from a different batch of concrete to determine fracture properties under monotonic loading by the size-effect method.

The specimens of different sizes, both for cyclic tests and companion monotonic tests, were geometrically similar in two dimensions, including the lengths of their

ACI Materials Journal, V. 88, No. 4, July-August 1991.
Received June 4, 1990, and reviewed under Institute publication policies.

Zdeněk P. Bažant, FACI, is Walter P. Murphy Professor of Civil Engineering at Northwestern University, Evanston Illinois, where he served as founding director of the Center for Concrete and Geomaterials. He is a registered structural engineer, a consultant to Argonne National Laboratory, and editor-in-chief of the ASCE Journal of Engineering Mechanics. *He is Chairman of ACI Committee 446, Fracture Mechanics; and member of ACI Committees 209, Creep and Shrinkage of Concrete; and 348, Structural Safety; and is Chairman of RILEM Committee TC 107 on Creep, of ASCE-EMD Programs Committee, and of SMiRT Division of Concrete and Nonmetallic Materials; and is a member of the Board of Directors of the Society of Engineering Science. Currently, he conducts research at the Technical University in Munich under Humboldt Award of U.S. Senior Scientist.*

Kangming Xu is a graduate research assistant in the Department of Civil Engineering at Northwestern University. He received his BS and MS from Wuhan University of Hydraulic and Electric Engineering, Wuhan, China.

notches. The thickness of all the specimens was the same (b = 1.5 in. = 38.1 mm). The beam depths were d = 1.5, 3, and 6 in. (38.1, 76.2, and 127 mm); the span was $L = 2.5d$; and the notch depth was $a_0 = d/6$ (Fig. 3).

The specimens were cast with the loaded side on top and demolded after 24 hr. Subsequently, the specimens were cured in a moist room with 95 percent relative humidity and 79 F (26.1 C) temperature until the time of the test. Just before the test, the notches were cut with a band saw. When tested, the specimens were 1 month old. During the test, the specimens were positioned upside down with the notch on top. The effect of specimen weight was negligible. During the cyclic tests (as well as the monotonic control tests), the laboratory environment had a relative humidity of about 65 percent and temperature about 78 F (25.6 C). The crack-mouth opening displacement (CMOD) was measured by a linear variable differential transformer (LVDT) gage supported on metallic platelets glued to the concrete.

In view of the difficulty of optical and other direct measurements, the crack length was measured indirectly, by the CMOD-compliance method. The validity of this method for concrete has recently been confirmed.[19,20] The compliance-calibration curve of the specimen (Fig. 4) was experimentally determined as follows:

1. Mark the notch lengths on the beam flank surface according to a logarithmic scale.
2. Cut the notch at midspan with a band saw.
3. Mount the LVDT gage and set up the specimen in the testing machine.
4. Apply the load at CMOD rate 0.0004 in./min and, after several load cycles between zero and maximum, record, with an x-y recorder, the plot of load versus CMOD, from which the specimen compliance is later calculated (the load is small enough so that no crack would start).
5. Remove the specimen from the machine, extend the notch by sawing a cut up to the next mark, and repeat the procedure. The sawing is admissible due to using a small enough load for which the fracture process zone is so small that it is entirely removed each time a cut to the next mark is made; therefore, after each cut, the specimen responds nearly the same way as a virgin notched specimen. An example of the relevant portion of the calibration curve of specimen compliance versus

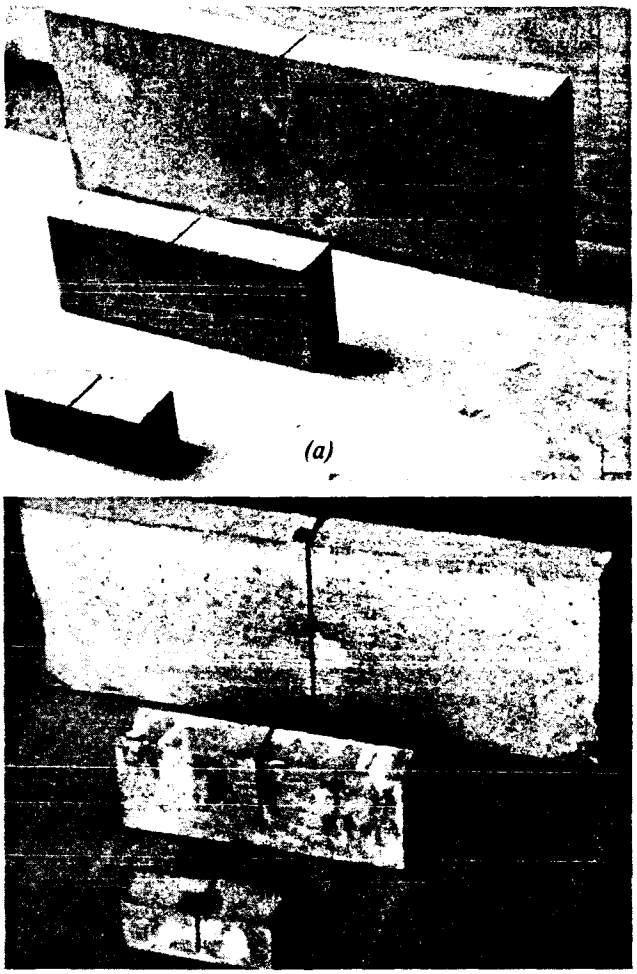

Fig. 1—(a) Fatigue fracture specimens of different sizes; and (b) use of fracture specimens in calibrating compliance

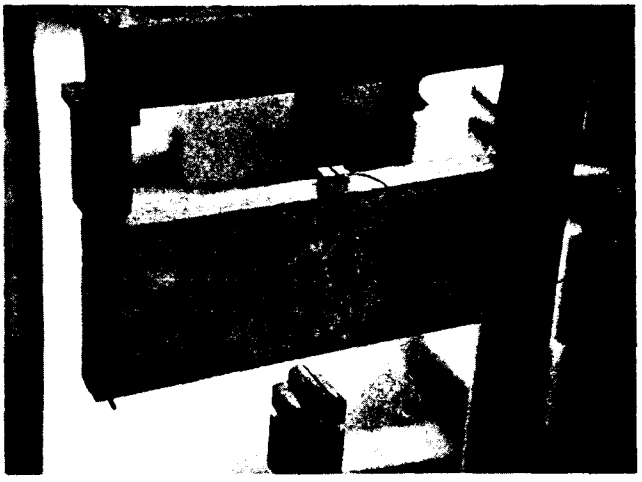

Fig. 2—Fatigue specimen with LVDT gage for crack mouth opening, being installed in the testing machine

the ratio of notch length to beam depth is seen in Fig. 4, which shows the measured data points as well as the curve of finite element results. Their deviation is within the range of normal experimental scatter in concrete testing.

In the cyclic tests, linear ramp load and frequency 0.033 to 0.040 Hz was used. In all the tests, the load

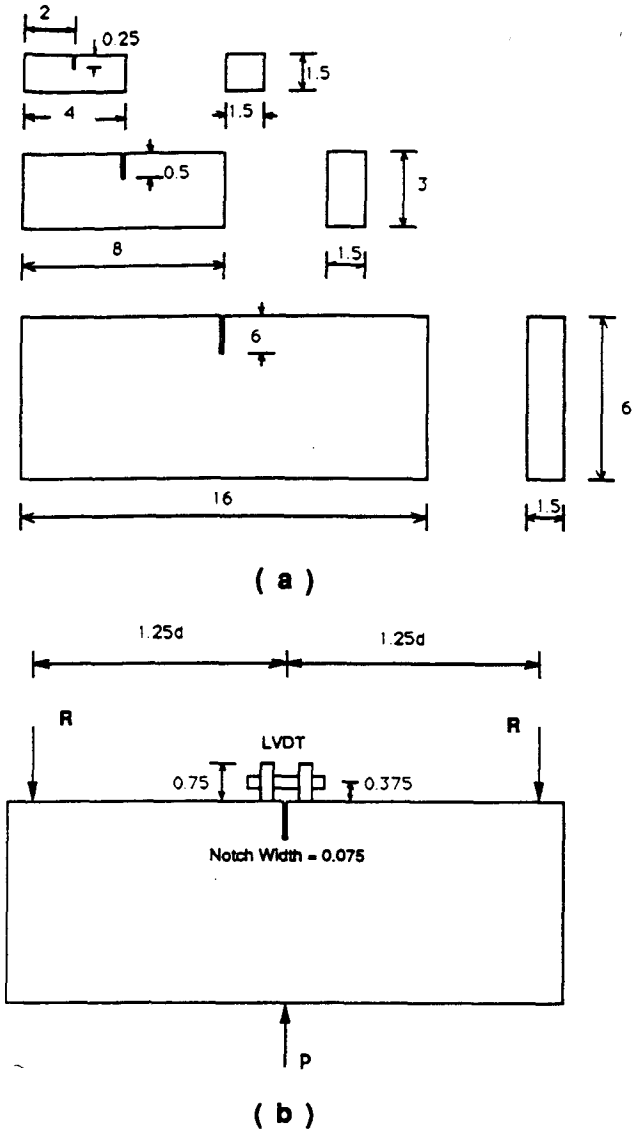

Fig. 3—Test specimen geometry

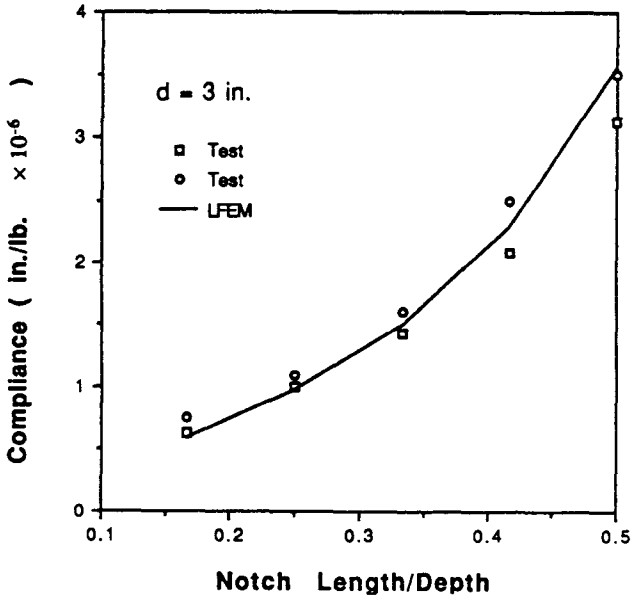

Fig. 4—Example of calculated and measured compliance calibration curve

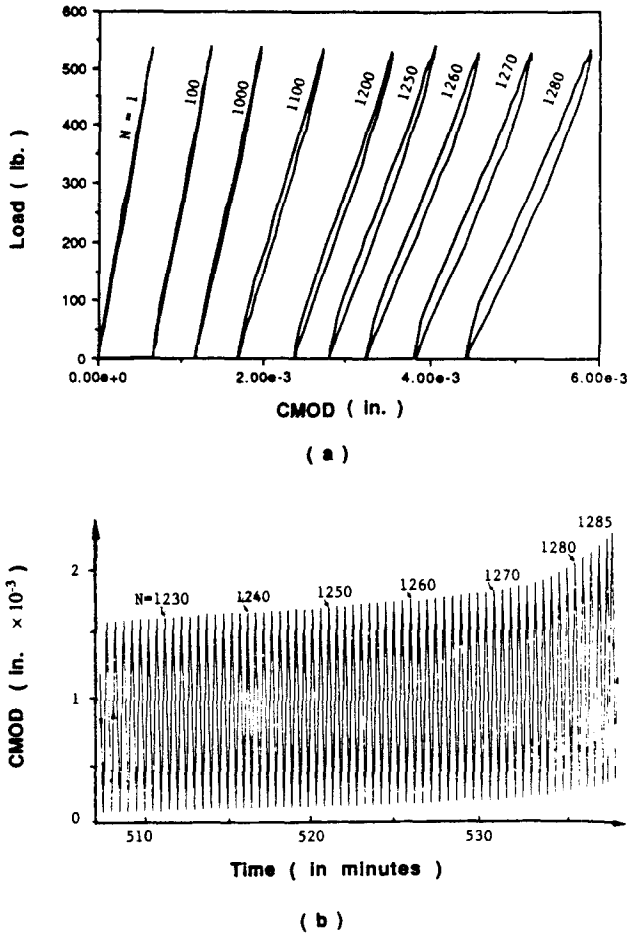

Fig. 5—(a) Load-CMOD record for one specimen of medium size; and (b) measured load history for the same specimen (CMOD = crack mouth opening displacement, in.)

minima were zero and the load maxima were constant and equal to 80 percent of the monotonic peak P_{max} load for a specimen of the same size and the same notch length. The first loading to $0.8P_{max}$ was to a pre-peak state.

TEST RESULTS

An automatic plotter was used to continuously record the load history [Fig. 5(a)] and the CMOD history [Fig. 5(b)] in each cycle (only the terminal part of these histories near failure is shown in Fig. 5). The effective crack length, representing the coordinate of the tip of an equivalent elastic crack, has been determined from the compliance given by the slope of the unloading segment of the measured load-CMOD curve, according to the compliance-calibration curve shown in Fig. 4. Based on the effective crack length, one can determine the equivalent stress intensity factor K_I^{eq}. The maximum loads measured in the companion monotonic tests are given in Table 1. The table also gives the values obtained previously[21] on the same type of concrete and the same specimens. The fact that these previous values were nearly identical confirms reproducibility. The measured curves of load P versus CMOD are shown in Fig. 6.

Table 1 — Measured maximum loads for monotonic loading

Tests	Depth, in.	Maximum load P, lb			Mean P, lb
		1	2	3	
Present tests	1.5	386	413	428	408
	3.0	669	649	694	671
	6.0	1190	1152	1154	1165
Tests of Bažant and Pfeiffer[21]	1.5	405	408	410	408
	3.0	677	706	698	698
	6.0	990	1040	1042	1024
	12.0	1738	1739	1750	1742

According to the fatigue fracture theory,[1,2] crack growth depends on the amplitude ΔK_I of the stress intensity factor K_I for the current effective (elastically equivalent) crack length a. As is well known

$$K_I = \frac{P f(\alpha)}{b\sqrt{d}} = \sigma_N \sqrt{d}\frac{f(\alpha)}{c_n},\ \alpha = \frac{a}{d} \qquad (1)$$

in which α = relative crack length, d = characteristic dimension of the specimen or structure, b = specimen thickness, P = load, and $f(\alpha)$ = function depending on specimen geometry, which can be obtained by elastic finite element analysis, and for typical specimen geometries is given in handbooks; for the present three-point bend specimens, $f(\alpha) = (1-\alpha)^{-3/2}(1 - 2.5\alpha + 4.49\alpha^2 - 3.98\alpha^3 + 1.33\alpha^4)$, as determined by curve-fitting of finite element results[22] and

$$\sigma_N = c_n P / bd \qquad (2)$$

where σ_N = nominal stress; and c_n = coefficient chosen for convenience, for example, so that σ_N would represent the maximum stress according to the bending theory formula for the ligament cross section; in that case $c_n = 3L/2(d - a_0)$ = constant for geometrically similar specimens of different sizes. If the crack length is very small (microscopic), i.e., $a \ll d$, then $K_I = \sigma_Y \sqrt{\pi a}$, where σ_Y is the local macroscopic stress calculated as if there were no crack, but in our case, due to the notch, the crack is not microscopic.

The fatigue test results are presented in Fig. 7, which shows the relative effective crack length $\alpha = a/d$ (calculated from the compliance data), as a function of the number N of cycles, for each of the six specimens tested (two of each size). From this figure, the measured points in the plot of $\log(\Delta a/\Delta N)$ versus $\log(\Delta K_I/K_{If})$ have been constructed, as shown in Fig. 8(a) for a series of three specimens, one of each size, and in Fig. 8(b) for both series, two specimens of each size. Here ΔK_I is the amplitude of the equivalent stress intensity factor calculated on the basis of the current effective crack length a (of course $\Delta K_I = K_I$ because the lower load limit is 0 in the present tests); ΔN represents the increments between the consecutive cycles number N = 10, 110, 210,...710, 760, 810, 820, 830,...900, 905, 910,...965, 966, 967,....974, and Δ_a are the corresponding increments of a. The small, medium, and large specimens failed at N = 974, 850, and 882, respectively, for the first group, and at N = 939, 1286, and 1083 for the second group. The units in Fig. 8 are in inches (25.4 mm) for a and in lb/in.$^{3/2}$ (1.099 N/cm$^{-3/2}$) for K_I.

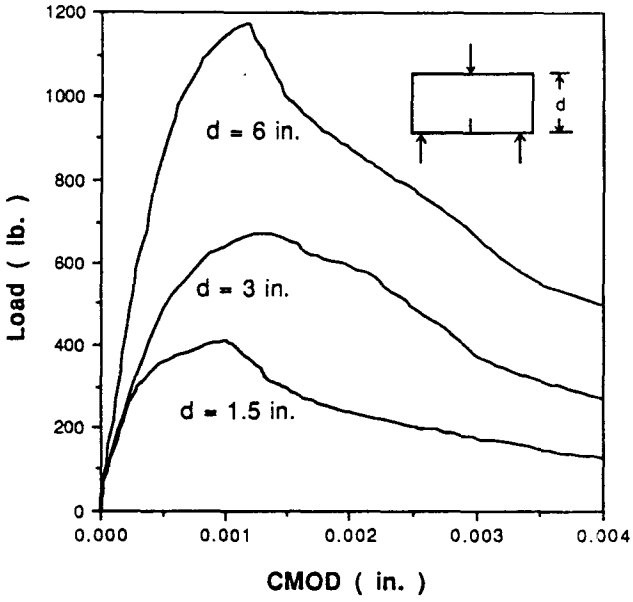

Fig. 6—Load-CMOD curves measured in monotonic loading of notched beam specimens of three sizes (1 in. = 25.4 mm; 1 lb = 4.45 N)

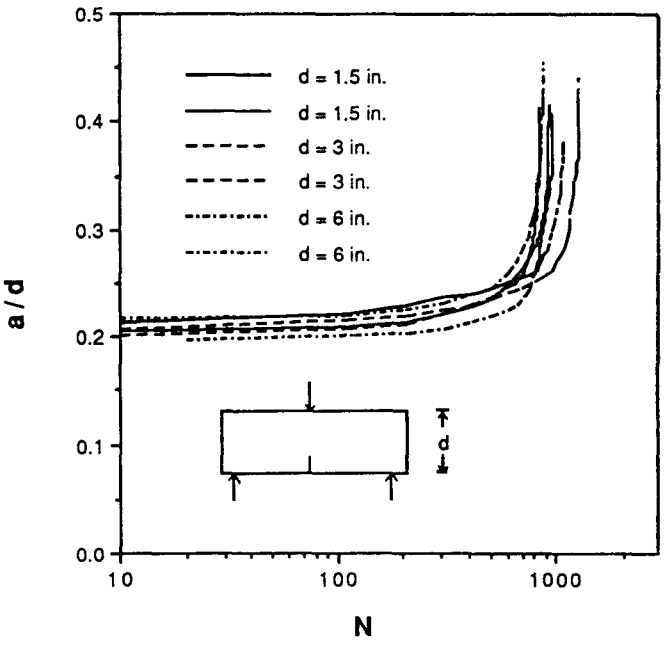

Fig. 7—Measured and calculated growth of the relative crack length with the number of cycles, for all six specimens (two for each size)

SIZE EFFECT IN PARIS LAW

As demonstrated extensively for metals, fatigue fracture follows approximately the empirical Paris law[17,18]

$$\frac{\Delta a}{\Delta N} = C\left[\frac{\Delta K_I}{K_{If}}\right]^n \qquad (3)$$

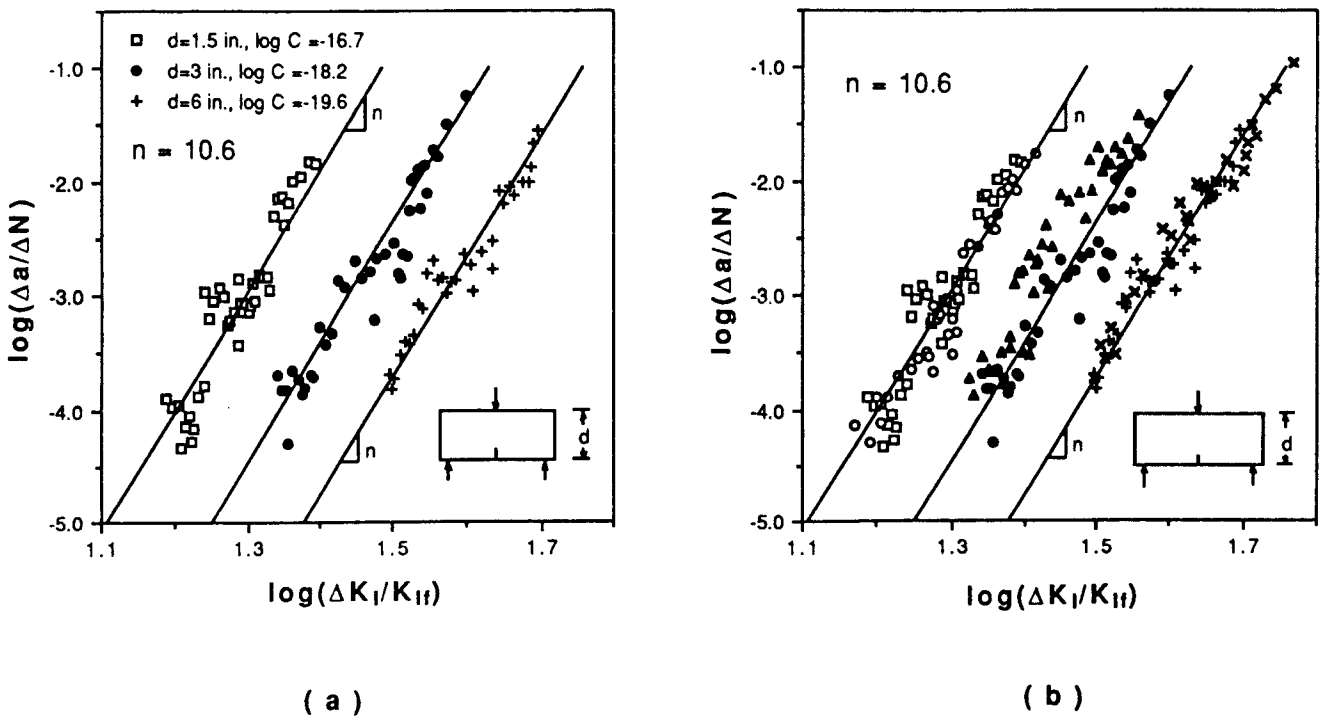

Fig. 8—Logarithmic plots of crack length increment per cycle versus the stress intensity factor amplitude, with independent regression lines for specimens of three sizes (a in inches)

in which C and n are empirical material constants; n is nondimensional and, for reasons of physical dimensions, K_{If} = constant = fracture toughness (which is introduced merely for convenience, so that coefficient C would have the dimension of length. Symbol Δ in Eq. (3) denotes the differences taken over one cycle or a sufficiently small number ΔN of cycles, so that $\Delta a/\Delta N$ would approximate the derivative da/dN. When the range of ΔK_I is very broad, the test results for metals deviate below the plot of Eq. (3) for very low ΔK_I and above it for very high ΔK_I,[1] but for a narrow enough range Eq. (3) is good for metals.

According to the Paris law, the plot in Fig. 8 would have to be a single inclined straight line of slope n. This is seen to be true for each specimen of each size [see Fig. 8(a)] from the slope and intercept of the regression line of the data points for each specimen. One gets n = 11.78, log$C$ = −40.2 (C given in inches) for the smallest size; n = 9.97, log$C$ = −36.0 for the medium size; and n = 9.27, log$C$ −34.8 for the largest size, with the overall average n = 10.57. The optimum fits by the straight lines of slope equal to this average slope are shown in Fig. 8. Fig. 8(b) shows the data for all six specimens (two of each size) compared to the same straight lines as in Fig. 8(a). These three fits are satisfactory, but there are great differences among the optimum C-values for the three lines for specimens of various sizes. So we must conclude that the Paris law is invalid for concrete in general.

This is not really a surprising result, in view of the well-known deviations of concrete behavior from linear elastic fracture mechanics (LEFM), whose applicability has been inherent to the previous applications of the Paris law. For monotonic loading, the first-order approximation of these deviations can be quite well described in terms of the size-effect law[23,24]

$$\sigma_N = B f_u (1 + \beta)^{-1/2}, \beta = d / d_0 \qquad (4)$$

Fig. 9(a) shows that B and d_0 are empirical constants characterizing both the material properties and specimen geometry; f_u is a measure of the tensile strength, e.g., $f_u = f_t'$ = direct tensile strength; σ_N = nominal strength = nominal stress at maximum (ultimate) load P_u, $\sigma_N = c_n P_u/bd$ [Eq. (2)]; and d_0 has the meaning of a transitional size (dimension) of the structure such that, for $d_0 \gg d_0$ (i.e., $\beta \gg 1$), failure is governed by LEFM while, for $d \ll d_0$ ($\beta \ll 1$), failure is governed by strength theory (or plasticity). For this reason, β is called the brittleness number.[21,25-27] Eq. (4), describing a transition from the size effect of plasticity (i.e., no size effect in strength) to the size effect of LEFM (i.e., the maximum possible size effect in strength), is only approximate, but the accuracy appears to be sufficient for the size range (ratio of minimum d to maximum d) up to about 1:20.

Due to deviations from LEFM, the critical value K_{Ic} of stress intensity factor K_I, at which the crack can propagate at monotonic loading, is not constant but depends on specimen size and geometry. An unambiguous definition, independent of size and geometry, can be given only for the extrapolation of K_{Ic} to infinite size.[21,25] Such extrapolated value is the fracture toughness K_{If} representing a true material property; K_{If} = lim K_{Ic} for $d \to \infty$. The corresponding fracture energy is $G_f = K_{If}^2/E$. (More generally, G_f could be defined as the limit of the critical value of Rice's J-integral for $d \to \infty$.) At infinite size, the specimen geometry cannot matter because (1) the fracture process zone occupies an infinitely small fraction of the specimen volume so that

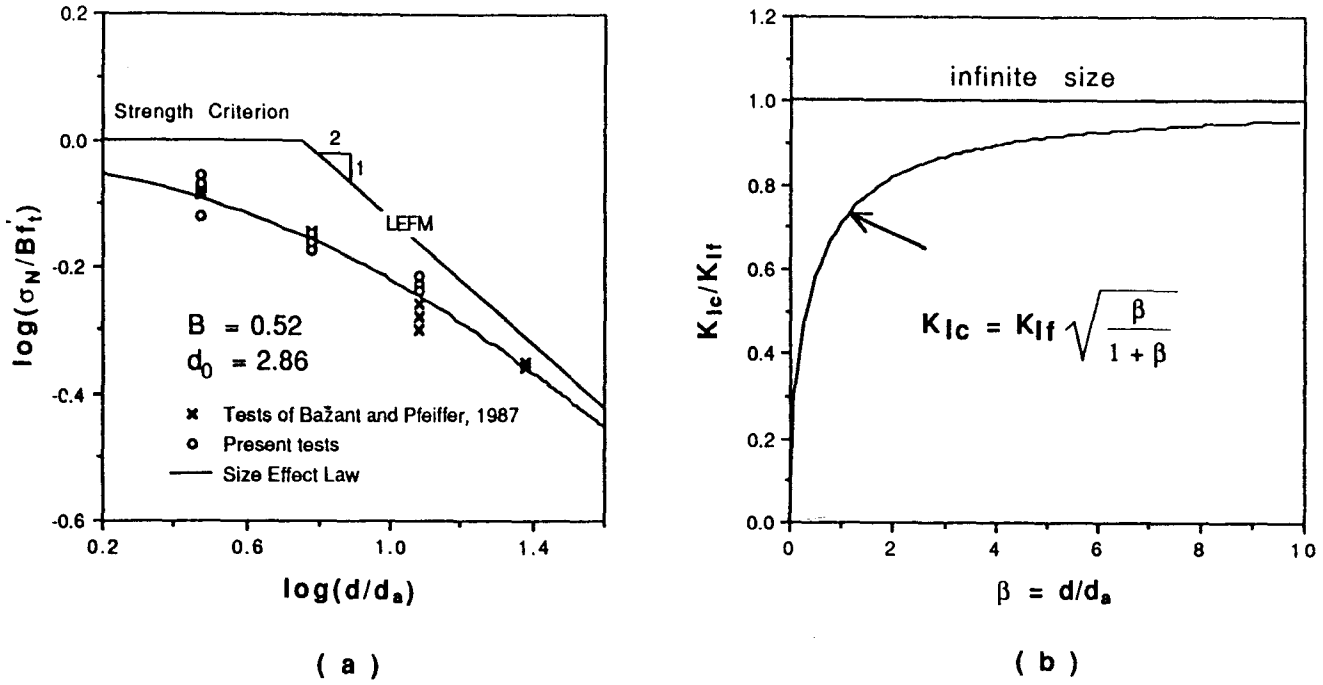

Fig. 9—Size-effect law for (a) nominal strength and (b) critical stress intensity factor

the whole specimen is in an elastic state, and (2) the near-tip asymptotic elastic field to which the fracture process zone is exposed at its boundary is the same for any specimen geometry.

To determine the size dependence of K_{Ic}, we first express K_{Ic} by substituting $P = P_u$ with $P_u = \sigma_N bd/c_n$ into Eq. (1). Then, substituting Eq. (4) for σ, we obtain [Fig. 9(b)]

$$K_{Ic} = \frac{B f_u \sqrt{\beta d_0}}{\sqrt{1+\beta}} \frac{f(\alpha_0)}{c_n} = K_{If}\left[\frac{\beta}{1+\beta}\right]^{1/2} \tag{5}$$

in which K_{If} is a constant expressed as

$$K_{If} = B f_u \sqrt{d_0} \frac{f(\alpha_0)}{c_n} \tag{6}$$

where we recognized that K_{If} is the fracture toughness as defined previously because it represents the limit of Eq. (4) for $d \to \infty$ or $\beta \to \infty$. Eq. (6)[21,25] means that the fracture toughness can be obtained from the size-effect law parameters B and d_0. These parameters, in turn, can be obtained if the values of $(f_u/\sigma_N)^2$, calculated from the measured peak values P_u of the curves in Fig. 6, are plotted versus d in Fig. 9(a). In this plot, the slope of the regression line is $1/Bd_0$, and the vertical axis intercept is 1/B. Linear regression of the peak load values from the present monotonic fracture tests provided $B = 0.520$, $d_0 = 2.86$ in. (72.6 mm), from which $K_{If} = 73.5$ lb/in.$^{3/2}$ (1.099 N/cm$^{-3/2}$).

How should the size effect be manifested in fatigue fracture? The monotonic fracture represents the limiting case of fatigue fracture as $\Delta K_I \to K_{Ic}$ at $N \to 1$. If the value of ΔK_I is close to K_{Ic}, $\Delta a/\Delta N$ must become very large while K_{Ic} must at the same time agree with the size-effect law for monotonic loading. This can be modeled by replacing in the Paris law [Eq. (3)] the constant fracture toughness K_{If} with the size-dependent equivalent fracture toughness K_{Ic} given by Eq. (5). So a generalized, size-adjusted Paris law may be written as

$$\frac{\Delta a}{\Delta N} = C\left[\frac{\Delta K_I}{K_{Ic}}\right]^n \tag{7}$$

The transition size d_0 in the size-effect law [Eq. (3)] applies only to peak-load states at monotonic loading. For fatigue fracture, however, it is unclear whether the value of the transitional size d_0, needed to calculate K_{Ic} [Eq. (5)], should be constant and the same as for monotonic fracture, or whether it should vary as a function of the ratio

$$\rho_K = \Delta K_I / K_{If} \tag{8}$$

Assuming $d_0 = 2.86$ in., the same as for monotonic fracture, the optimum fit of the present test data by the size-adjusted Paris law [Eq. (7)] is shown in Fig. 10(a) and (b) for the small, medium, and large specimens by the dashed straight lines. As can be seen, the fit has improved substantially compared to Fig. 8(a) and (b), but not enough. This finding means that the transitional size d_0 cannot be constant but must depend on ρ_K.

Assume that, for the present tests in which $\rho_K = 0.8$, the value of d_0 is 28.6 in., i.e., 10 times larger. Then the optimum fit of the present test data becomes as shown by the three straight lines in Fig. 11(a) and (b). The closeness of fit is now satisfactory. (That the factor of 10 happens to achieve a good fit of the data is of course merely by chance.)

According to Eq. (7), if $\log(\Delta a/\Delta N)$ is plotted against $\log(\Delta K_I/K_{Ic})$, the data points for the specimens of all

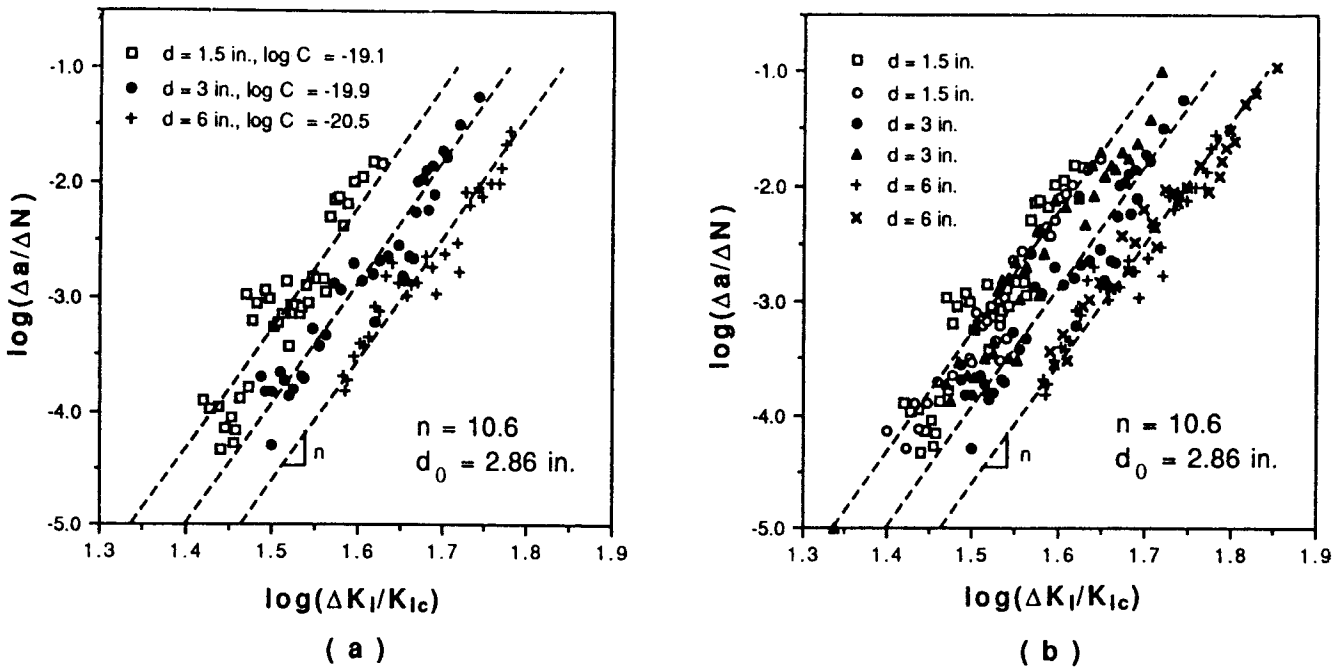

Fig. 10—Logarithmic plot of crack length increment per cycle versus the size-adjusted crack length amplitude, keeping the same d_0 *as in monotonic tests (left—one, and right—two specimens of each size)*

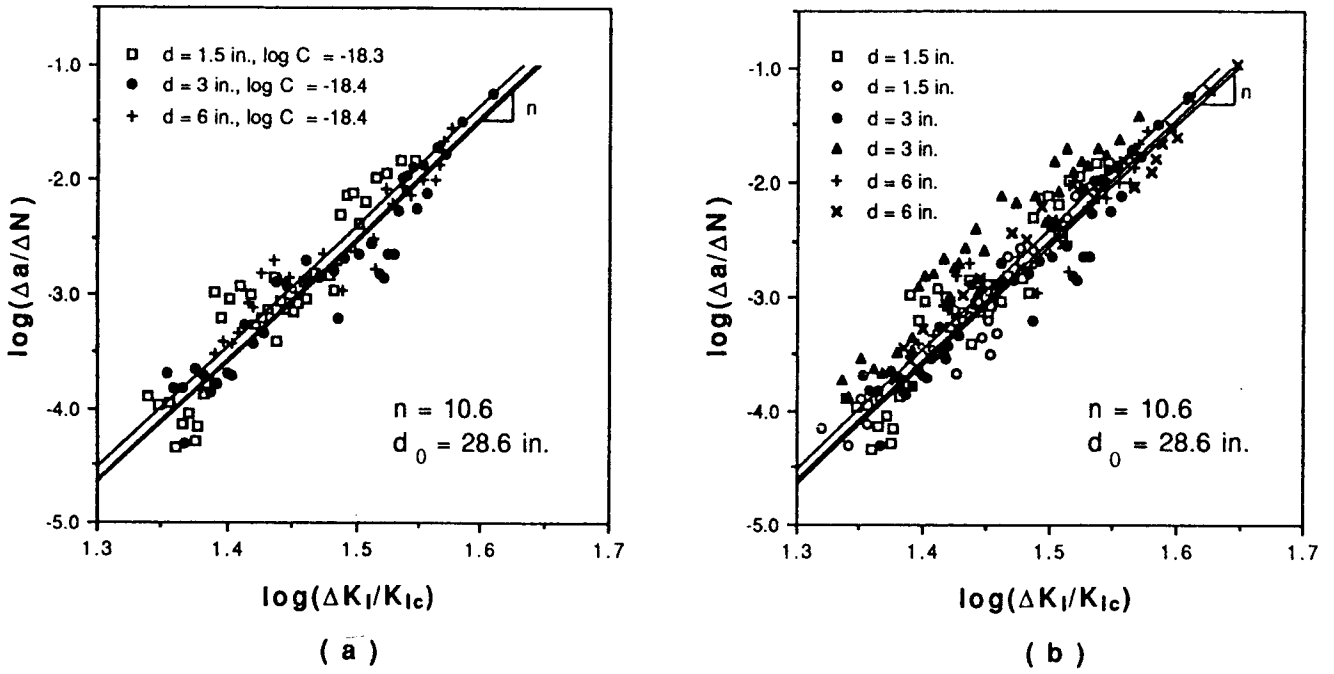

Fig. 11—Logarithmic plot of crack length increment per cycle versus the size-adjusted crack length amplitude, with transition size d_0 *10 times larger*

sizes should have a common regression line. Fig. 12 confirms that for d_0 = 28.6 in.; this is indeed approximately so.

As shown,[26,27] d_0 is proportional to the effective length of the fracture process zone. So the value of d_0 deduced from the present tests implies that the fracture process zone at load cycling with amplitude 80 percent of the maximum monotonic load should be about 10 times larger than it is for monotonic loading. Although the factor 10 might be too large to still accept equivalent LEFM calculations for the present size specimens, it nevertheless appears that the fracture process zone is greatly enlarged by load cycling.

CRACK GROWTH DEPENDENCE ON NOMINAL STRESS

Expressing ΔK_I according to Eq. (1), the unadjusted Paris law [Eq. (3)] may be written in terms of the amplitude $\Delta\sigma_N$ of the nominal stress

$$\frac{\Delta a}{\Delta N} = \overline{C}\,(\sqrt{\beta}\,\Delta\sigma_N)^n, \overline{C} = C\left[\sqrt{d_0}\,\frac{f(\alpha)}{c_n K_{If}}\right]^n \qquad (9)$$

where $\overline{C}$ is a constant if the specimens are geometrically similar, and $\beta = d/d_0$. Likewise, after expressing ΔK_I in Eq. (7) from Eq. (1), the size-adjusted Paris law [Eq. (7)] may also be written in terms of the nominal stress amplitude

$$\frac{\Delta a}{\Delta N} = \overline{C}\,(\sqrt{1+\beta}\,\Delta\sigma_N)^n \tag{10}$$

For very small specimen sizes $d \ll d_0$, this law simplifies as

$$\frac{\Delta a}{\Delta N} = \overline{C}\,(\Delta\sigma_N)^n \tag{11}$$

i.e., the size effect in fatigue fracture disappears. On the other hand, for very large sizes, $d \gg d_0$, Eq. (10) asymptotically approaches Eq. (9), and the size effect becomes the strongest possible.

The present data for the first series of fatigue specimens of three sizes (one specimen per size), already shown in Fig. 8(a), 10(a), and 11(a), are now plotted in Fig. 13(a) with $\log\Delta\sigma_N$ as the abscissa, and in Fig. 13(b) with the logarithm of the size-adjusted nominal stress amplitude as the abscissa. The three straight regression lines predicted by Eq. 11 are also drawn.

Comparison of Fig. 13(a) with Fig. 8, 10, and 11 reveals that, in terms of the nominal stress amplitude, the effect of size is much weaker than in terms of the stress intensity factor amplitude. This agrees with the conventional wisdom that concrete structures are relatively insensitive to fatigue. But for a sufficiently large size this ceases to be true.

The foregoing observation is of course incidental. It is due to the fact that all the specimens tested were relatively small. According to the size-effect law, the effect of size on the nominal strength vanishes when the size is very small, and is maximum when the size is very large. The opposite is true for the size dependence of

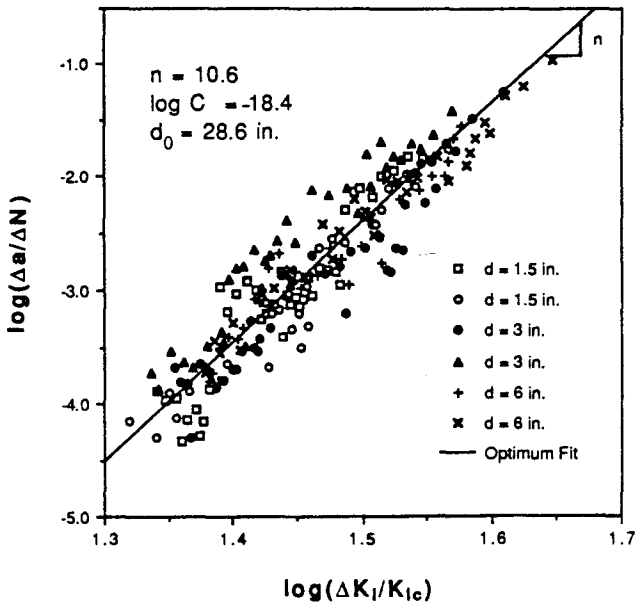

Fig. 12—Logarithmic plots of crack length increment per cycle versus the amplitude of size-adjusted stress intensity factor, two specimens of each of three sizes, and optimum fit by the size-adjusted Paris law [Eq. (7)]

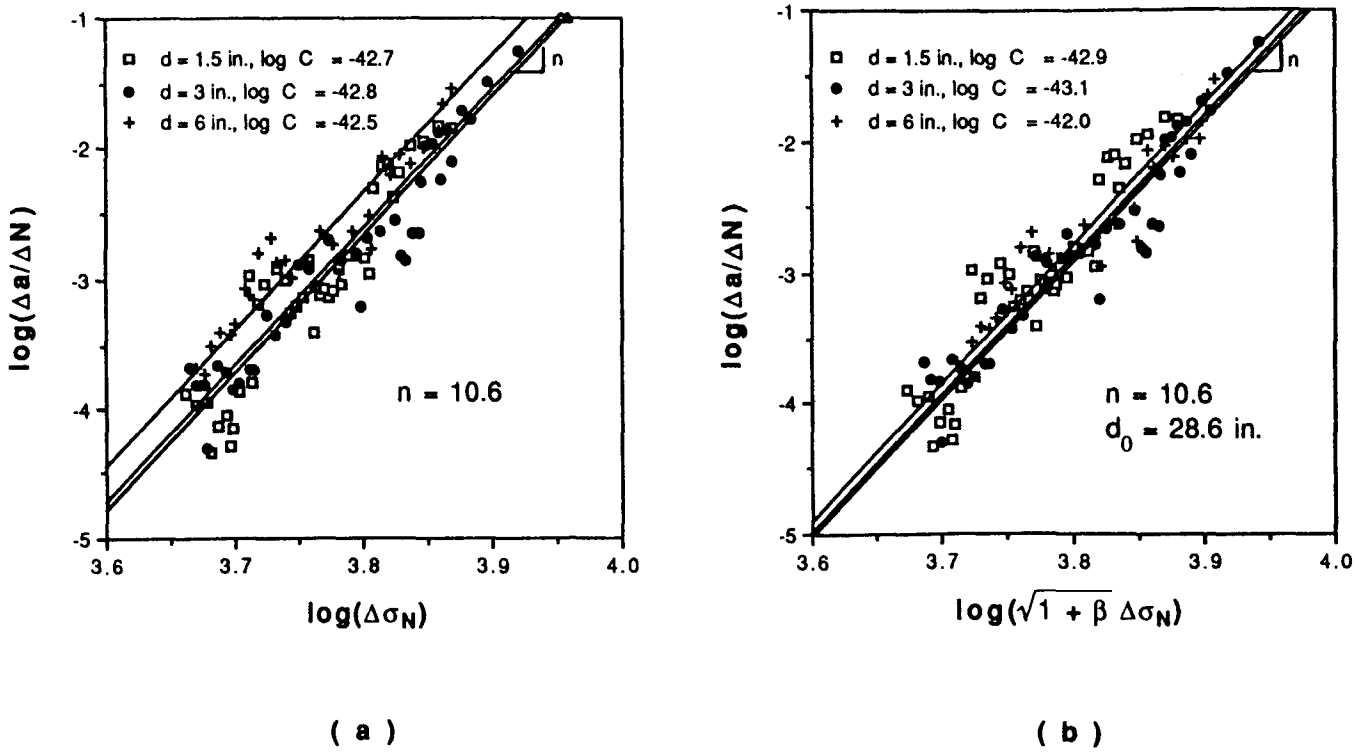

Fig. 13—Logarithmic plots of crack length increment per cycle versus nominal stress amplitude (left—without, and right—with size adjustment)

the stress intensity factor required for fracture growth [Eq. (4) and (7) and Fig. 7]. Thus, according to the present theory, the size effect in Fig. 13 should become very large, and in Fig. 8, 10, and 11 very small, when the specimen or structure is very large. For large structures, fatigue is better characterized in terms of the stress intensity factor amplitude, while for small structures, fatigue is better characterized in terms of the nominal stress amplitude. [Note that a good absolute measure of structure size is its brittleness number—the structure is very large if $\beta \gg 1$ and very small if $\beta \ll 1$ (Reference 21)].

Recall from Fig. 8, 10, and 11 that the larger the size, the smaller the crack length increment per cycle for the same stress intensity factor amplitude. For the same nominal stress amplitude, though, the larger the size, the larger the crack length increment per cycle (see Fig. 13). The last property is the same as in monotonic fracture—a size effect in the usual sense of a weakening of the structure with an increase of its size.

CRACK LENGTH VERSUS NUMBER OF CYCLES

It is also interesting to integrate Eq. (3). Replacing Δ with d, substituting $da = d_0 d\alpha$, and separating the variables gives $N = \int (\Delta K_I)^{-n} d\alpha \; d_0/C$. Then, by substituting Eq. (1), the following is obtained

$$N = (d_0/C)(b\sqrt{d}/P)^n \int [f(\alpha)]^{-n} d\alpha \qquad (12)$$

Numerical integration yields the three curves of the relative crack length α versus the number of cycles plotted in Fig. 7 for the three specimen sizes. As can be seen, these curves agree with the measurements relatively well. This again confirms that fracture mechanics is applicable, despite the fact that the size effect in terms of the nominal stress is quite mild in the present tests.

CONCLUSIONS

1. The Paris law for fatigue fracture is applicable to concrete. But for structures with macroscopic (large) cracks this is so only for one size of the specimen or structure or, asymptotically, for very large sizes. Otherwise, a modification of this law is required.

2. The Paris law may be adjusted for the size effect by combining it with the size-effect law proposed[23] for nominal strength in monotonic loading. This leads to a law in which the crack length increment per cycle is a power function of the amplitude of a size-adjusted stress intensity factor.

3. The size-adjusted Paris law is corroborated by the measurements of crack length growth due to fatigue loading of repeatedly loaded notched specimens of size range 1:4. The calculated growth of the crack length with the number of cycles also agrees with tests.

4. The fatigue crack growth can also be represented as a function of the nominal stress amplitude and the brittleness number. In the latter form, the size effect vanishes for very small structures, while in terms of the stress intensity factor amplitude it vanishes for very large structures. For sufficiently large structures, fatigue is better characterized in terms of the stress intensity factor amplitude, whereas for small structures fatigue is better characterized in terms of the nominal stress amplitude.

5. The transitional size, separating predominantly brittle failures from predominantly ductile (plastic or strength-governed) failures, appears to be much larger (roughly 10 times larger) for cyclic loading than it is for monotonic loading. Consequently, the brittleness number for a structure under cyclic loading is much smaller than it is for monotonic loading.

6. It must be emphasized that the scope of the present tests has been insufficient to check whether the foregoing conclusions are also valid when: (1) the stress intensity factor amplitude is varied; (2) the lower limit of the cyclic load is not zero; (3) the number of cycles per minute is varied; and (4) different specimen geometries and notch lengths are considered.

ACKNOWLEDGMENT

Partial financial support has been received for development of the theory from AFOSR Contract F49620-87-C-0030DEF with Northwestern University, and for experiments from NSF Science and Technology Center for Advanced Cement-Based Materials at Northwestern University (NSF Grant DMR 880-8432).

REFERENCES

1. Kanninen, M. F., and Popelar, C. H., *Advanced Fracture Mechanics,* Oxford University Press, 1985.

2. Broek, D., *Practical Use of Fracture Mechanics,* Kluwer Academic Publishers, Boston, 1988.

3. Barsom, J. M., and Rolfe, S. T., *Fracture and Fatigue Control in Structures: Applications of Fracture Mechanics,* Prentice-Hall, Englewood Cliffs, 1987.

4. Lawn, B. R.; Anstis, G. R.; Dabbs, T. P.; and Marshall, D. B., "Fatigue Analysis of Brittle Materials Using Indentation Flaws .1. General Theory," *Journal Of Materials Science,* V. 16, No. 10, 1981, pp. 2846-2854.

5. Cook, R. F.; Fairbanks, C. J.; and Lawn, B. R., "Microstructure-Strength Properties in Ceramics .1. Effect of Crack Size on Toughness, and .2. Fatigue Relations," *Journal* American Ceramic Society, V. 68, No. 11, 1985, pp. 604-623.

6. Ritchie, R. O., "Mechanisms of Fatigue Crack-Propagation in Metals, Ceramics and Composites—Role of Crack Tip Shielding," *Materials Science and Engineering,* V. 103, No. 1, 1988, pp. 15-28.

7. Nordby, Gene M., "Fatigue of Concrete—A Review of Research," ACI JOURNAL, *Proceedings* V. 55, No. 2, Aug. 1958, pp. 191-219.

8. Murdock, John W., and Kesler, Clyde E., "Effect of Range of Stress on Fatigue Strength of Plain Concrete Beams," ACI JOURNAL, *Proceedings* V. 55, No. 2 , Aug. 1958, pp. 221-231.

9. Stelson, Thomas E., and Cernica, John N., "Fatigue Properties of Concrete Beams," ACI JOURNAL, *Proceedings* V. 55, No. 2, Aug. 1958, pp. 255-259.

10. Hilsdorf, Hubert K., and Kesler, Clyde E., "Fatigue Strength of Concrete under Varying Flexural Stresses," ACI JOURNAL, *Proceedings* V. 63, No. 10, Oct. 1966, pp. 1059-1075.

11. Kaplan, M. F., "Flexural and Compressive Strength of Concrete as Affected by the Properties of Concrete Aggregates," ACI JOURNAL, *Proceedings* V. 55, No. 11, May 1959, pp. 1193-1208.

12. Baluch, M. H.; Qureshy, A. B.; and Azad, A. K., "Fatigue Crack Propagation in Plain Concrete," *Fracture of Concrete and Rock, SEM/RILEM International Conference,* Shah, S. P., and Swartz, S. E., Eds. (Houston, June 1987), Springer-Verlag, New York, 1989, pp. 80-87.

13. Perdikaris, P. C., and Calomino, A. M., "Kinetics of Crack Growth in Plain Concrete," *Fracture of Concrete and Rock,*

SEM/RILEM International Conference, Shah, S. P., and Swartz, S. E., Eds. (Houston, June 1987), Springer-Verlag, New York, 1989, pp. 64-69.

14. Suresh, S.; Tschegg, E. K.; and Brockenbrough, J. R., "Fatigue Crack Growth in Cementitious Materials under Cyclic Compressive Loads," *Cement and Concrete Research,* V. 19, No. 5, Sept. 1989, pp. 827-833.

15. Suresh, S., "Fatigue Crack Growth in Cementitious Solids under Cyclic Compression: Theory and Experiments," *Fracture of Concrete and Rock: Recent Developments,* Elsevier Applied Science, London and New York, Sept. 1989, pp. 162-172.

16. Zhang, Binsheng; Zhu, Zhaohung; and Wu, Keru, "Fatigue Rupture of Plain Concrete Analyzed by Fracture Mechanics," *Fracture of Concrete and Rock, SEM/RILEM International Conference,* Shah, S. P., and Swartz, S. E., Eds. (Houston, June 1987), Springer-Verlag, New York, 1989, pp. 58-63.

17. Paris, P. C.; Gomez, M. P.; and Anderson, W. E., "Rational Analytic Theory of Fatigue," *Trend in Engineering,* V. 13, No. 1, Jan. 1961.

18. Paris, P. C., and Erdogan, F., "Critical Analysis of Propagation Laws," *Transactions of ASME, Journal of Basic Engineering,* V. 85, 1963, pp. 528-534.

19. Swartz, S. E., and Go, C. G, "Validity of Compliance Calibration to Cracked Beams in Bonding," *Journal of Experimental Mechanics,* V. 24, No. 2, June 1984, pp. 129-134.

20. Perdikaris, P. C.; Calomino, A. M.; and Chudnovsky, A., "Effect of Fracture on Fracture Toughness of Concrete," *Journal of Engineering Mechanics,* V. 112, No. 8, Aug. 1986, pp. 776-791.

21. Bažant, Zdeněk P., and Pfeiffer, Phillip A., "Determination of Fracture Energy from Size Effect and Brittleness Number," *ACI Materials Journal,* V. 84, No. 6, Nov.-Dec. 1987, pp. 463-480.

22. Gettu, R.; Bažant, Z. P.; and Karr, M. E., "Fracture Properties and Brittleness of High Strength Concrete," *Report* No. 89-10/B627f, Center for Advanced Cement-Based Materials, McCormick School of Engineering and Applied Science, Northwestern University, Oct. 1989.

23. Bažant, Z. P., "Size Effect in Blunt Fracture: Concrete, Rock, Metal," *Journal of Engineering Mechanics,* ASCE, V. 110, No. 4, Apr. 1984, pp. 518-535.

24. Bažant, Z. P., "Mechanics of Distributed Cracking," *Applied Mechanics Reviews,* V. 39, No. 5, May 1986, pp. 675-705.

25. Bažant, Zdeněk P., "Fracture Energy of Heterogeneous Materials and Similitude," *Fracture of Concrete and Rock, SEM/RILEM International Conference,* Shah, S. P., and Swartz, S. E., Eds. (Houston, June 1987), Springer-Verlag, New York, 1989, pp. 229-241.

26. Bažant, Z. P., and Kazemi, M. T., "Determination of Fracture Energy, Process Zone Length and Brittleness Number from Size Effect, with Application to Rock and Concrete," *Report* No. 88-7/498d, Center for Concrete and Geomaterials, Technological Institute, Northwestern University, July 1988.

27. Bažant, Z. P., and Kazemi, M. T., "Size Effect in Fracture of Ceramics and Its Use to Determine Fracture Energy and Effective Process Zone Length," *Report* No. 89-6/498s, Center for Advanced Cement-Based Materials, McCormick School of Engineering and Applied Science, Northwestern University, June 1989.